

Journal of Nanophotonics

Nanophotonics.SPIEDigitalLibrary.org

Impact of channel scaling on performance of single SiC nanowire UV photodetector

Ali Uzun
Kasif Teker

SPIE.

Ali Uzun, Kasif Teker, "Impact of channel scaling on performance of single SiC nanowire UV photodetector," *J. Nanophoton.* **13**(2), 026003 (2019), doi: 10.1117/1.JNP.13.026003.

Impact of channel scaling on performance of single SiC nanowire UV photodetector

Ali Uzun and Kasif Teker*

Istanbul Sehir University, Department of Electrical and Electronics Engineering, Istanbul, Turkey

Abstract. We have investigated the channel length dependence of the key performance parameters, such as speed, responsivity, external quantum efficiency (EQE), and responsivity–bandwidth product, of the silicon carbide nanowire-based ultraviolet (UV) photodetector devices with different channel lengths ranging from 120 to 800 nm. The device with the shortest channel length of 120 nm at low bias voltage of 0.5 V exhibited very high responsivity and EQE of 7.73×10^3 A/W and $7.77 \times 10^4\%$, respectively, under illumination to 254-nm UV light. Our experiments revealed that reduction in channel length resulted in significant enhancement in speed, responsivity, EQE, and responsivity–bandwidth product of the photodetector. This study suggests that scaling down in channel length could enable the development of high-speed and sensitive photodetector devices for emerging nanophotonic and nanoelectronic applications capable of operating at low voltages. © 2019 Society of Photo-Optical Instrumentation Engineers (SPIE) [DOI: [10.1117/1.JNP.13.026003](https://doi.org/10.1117/1.JNP.13.026003)]

Keywords: channel scaling; silicon carbide nanowire-based ultraviolet photodetector; low-voltage operation; responsivity.

Paper 19008 received Jan. 21, 2019; accepted for publication Apr. 8, 2019; published online Apr. 23, 2019.

1 Introduction

One-dimensional (1-D) nanostructures with their high sensitivity due to large surface-to-volume ratio and high crystal quality are considered as one of the most promising candidates to develop nanoscale electronic and optoelectronic devices. SiC nanowires, a wide bandgap semiconductor, merge particular features of 1-D nanostructures with remarkable inherent properties of SiC and enable one to realize advanced devices and sensors, such as field-effect transistors,^{1,2} solar cells,^{3,4} Schottky diodes,^{5,6} and photodetectors^{7–11} that can operate at high frequency, high power, and harsh environment. Among these applications, ultraviolet (UV) photodetectors have drawn tremendous interest due to its wide potential usage ranging from military applications, such as defense systems and UV communication,^{5,12} to civil applications, such as food and drink industry, chemical, and medical industry.^{13,14} Moreover, SiC is an excellent semiconductor for UV photodetection due to its outstanding long-term stability even under high-intensity UV radiation and at high operating temperatures.

To develop more sensitive, reliable, and power efficient optoelectronic devices, considerable efforts have been made by experimenting with variety of semiconductor nanomaterials, such as metal oxides (ZnO and TiO₂),^{10,15,16} III-nitrides (GaN and AlN),^{8,17} In₂Se₃,⁹ and SiC.^{10,11} For instance, Boruah et al.⁷ synthesized highly dense ZnO nanowires on graphene foam substrate as a UV photodetector with a rise and decay times of 9.5 and 38 s, respectively, and gain of 2490.8% at 5-V bias voltage. Weng et al.⁸ fabricated a metalorganic chemical vapor deposition (MOCVD) grown GaN nanowire UV photodetector with an external quantum efficiency (EQE) of ~100% at 5-V bias voltage. A single In₂Se₃ nanowire-based photodetector was reported with response times of 0.3 s, responsivity (R_λ) of ~89 A/W, and EQE of 22,000% at operating bias voltage of 3 V.¹³ Ko et al.¹⁸ reported a compact bipolar junction phototransistor with a high current gain of 53.6, bandwidth of 7 GHz, and responsivity of 9.5 A/W using a single crystalline

*Address all correspondence to Kasif Teker, E-mail: kasifteker@sehir.edu.tr

indium phosphide nanopillar directly grown on a silicon substrate. Going et al.¹⁹ reported a germanium gated N-type metal-oxide-semiconductor phototransistor integrated on a silicon-on-insulator substrate with a responsivity of over 18 A/W at 1550 nm with 583 nW of incident light. Additionally, Aldalbahi et al.¹⁰ prepared a SiC film-based UV photodetector with R_λ of 0.18 A/W and EQE of 86%. In fact, very few studies have been reported on silicon carbide nanowire-based ultraviolet photodetector (SiCNW-UVPD). Teker¹¹ designed a photodetector by utilizing SiCNW with a rise time of 3 s and decay time of 5 s under 254-nm UV light illumination at bias voltage of 2 V.

Herein, we investigate, for the first time to the authors' knowledge, the scaling effect of channel length on key performance parameters, such as rise and decay time, responsivity, EQE, and responsivity–bandwidth product of the SiCNW-UVPDs. The photodetection characteristics of three devices with varying channel length of 120, 460, and 800 nm have been systematically investigated under 254-nm UV light illumination at various bias voltages ranging from 0.5 to 2 V with a step size of 0.5 V. The study has shown that the SiCNW-UVPDs have high R_λ of 7.73×10^3 A/W and EQE of $7.77 \times 10^4\%$ at low operating voltage of 0.5 V with the shortest channel length of 120 nm. Channel length scaling can provide new insights to realize the development of high sensitivity, reliable, and low power consuming UV photodetector devices, which can be used in nanoscale electronic and optoelectronic applications.

2 Experimental Details

SiC nanowires were synthesized in a horizontal RF-induction heated MOCVD reactor on a SiO₂/Si substrate at 1100°C with hexamethyldisilane as a source precursor. Crystal structure of the nanowires has been characterized by x-ray diffraction (XRD). Surface morphology of the nanowires has been observed by scanning electron microscopy (SEM). To investigate the photodetection characteristics of the MOCVD-grown SiC nanowires, single SiCNW-based multiple UV photodetector devices were fabricated with varying channel size. First, SiCNWs in isopropyl alcohol solution were deposited on a highly doped SiO₂/Si substrate with an oxide layer of 300 nm. Then, the electrodes (Cr/Au: 3/100 nm) were defined by e-beam lithography for the channel length ranging from 120 to 800 nm followed by metal deposition through e-beam evaporation. O₂ plasma treatment was carried out to remove the possible resist/residue on the fabricated SiCNW devices. Before the measurements, an annealing process was performed at 400°C for 5 min under 5 standard cubic centimeters per minute of Ar flow in a chamber to improve the quality of the nanowire–electrode contact. The photocurrent measurements including I – V curves and photocurrent–time responses ($I_{ds} - t$) have been carried out under 254-nm wavelength UV light (UVGL-58 handheld UV lamp) on a probe station using a Keithley 2634B sourcemeter. The UV lamp intensity and the distance between the UV light source and the SiCNW-UVPDs were 1.35 mW/cm² and 3.6 cm, respectively.

3 Results and Discussions

A typical SEM image of the SiCNWs grown at 1100°C with catalyst Ni nanoparticles on a SiO₂/Si substrate is shown in Fig. 1(a). The image reveals that SiC nanowires have diameters ranging from 40 to 70 nm and lengths up to 50 μm. XRD analysis was carried out to examine crystal structure of the nanowires and the pattern is shown in Fig. 1(b). Figure 1(b) exhibits one strong peak at 35.6 deg and one weak peak at 59.9 deg corresponding to SiC (111) and SiC (220), respectively. The diffraction pattern indicates that 3C-SiC is the main crystalline phase of the nanowires (JCPDS card no. 29-1129). Following the morphological and structural characterization of the SiCNWs, photodetector devices were configured on a highly doped Si substrate coated with 300-nm dry SiO₂ with varying channel lengths from 120 to 800 nm. Figure 2(a) shows SEM images (with an inset) of the fabricated SiCNW-UVPDs. Two of these devices with the channel lengths of 120 and 460 nm were fabricated on the same SiC nanowire, and the third device with the channel length of 800 nm was fabricated on another SiC nanowire. All the devices have been fabricated on the nanowires with 65-nm diameter from the same growth run to ensure the same crystal quality. Figure 2(b) shows a schematic view of the measurement setup of the SiCNW-UVPDs.

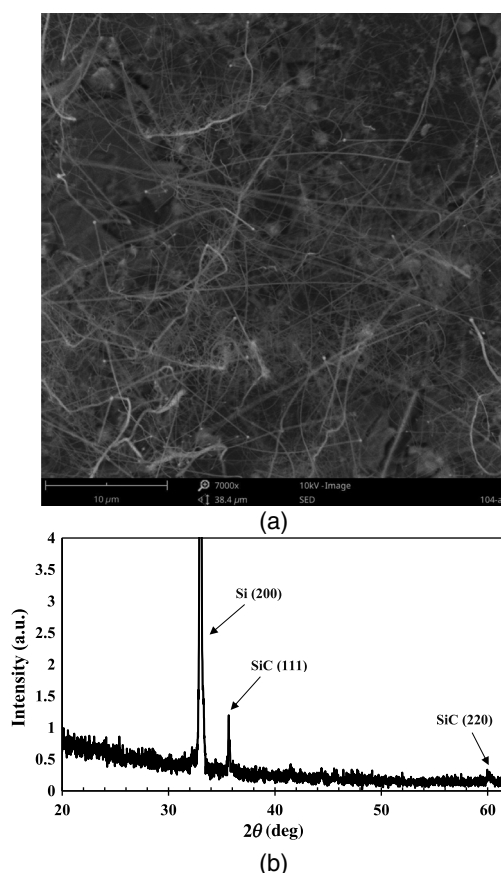
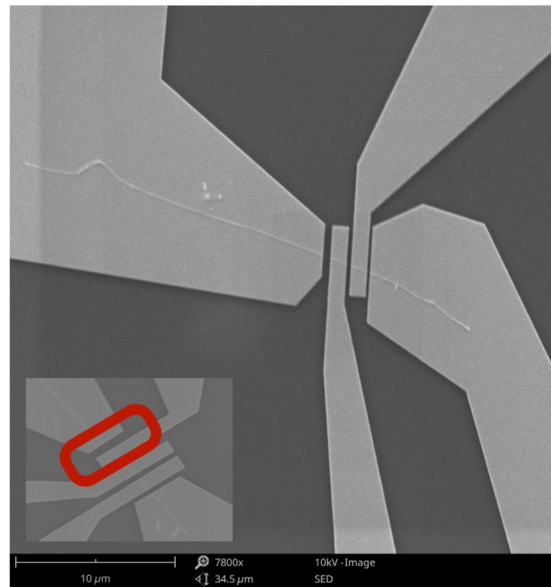


Fig. 1 (a) An SEM image of the SiC nanowires on a SiO_2/Si substrate (scale bar is $10 \mu\text{m}$) and (b) XRD pattern of the SiCNWs with zinc blende crystal structure.

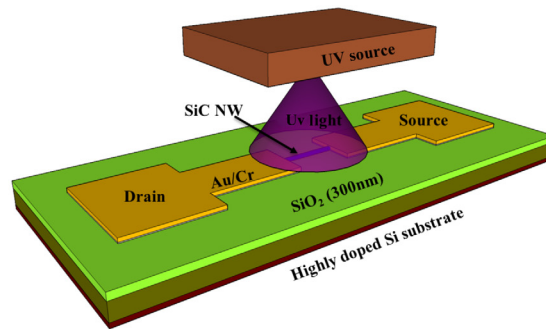
The I - V characteristics of the single SiCNW-UVPD device were conducted both in dark and 254-nm UV light exposure, as shown in Fig. 3. The measurements have been conducted by a voltage sweep at the drain-source voltage (V_{ds}) from -1.5 to 1.5 V at a gate voltage of 0 V. The device is a metal-semiconductor-metal type and reveals a high photocurrent to the UV exposure. It can be stated that the SiCNW-UVPD has high sensitivity to the UV light with a high photocurrent-to-dark current ratio (~ 2 at 1.5 V). It is worth mentioning that the nanowires have p -type behavior as determined from the high drain-source current for the negative gate voltages in dark conditions.²⁰

Next, photocurrent-time response dynamics of the SiCNW-UVPD device with 120-nm channel length under 254-nm UV light irradiation at different bias voltages (0.5 , 1 , 1.5 , and 2 V) have been recorded for three consecutive cycles of ON (10 s) and OFF (20 s) states, as shown in Fig. 4(a). After each ON-OFF cycle, the UV detector shows fast reversibility by returning the initial current value (I_{dark}), which indicates that the UV detector has good reversibility as well as repeatability. It is important to point out that the photocurrent (I_{ph}), which is defined as $I_{\text{ph}} = I_{\text{light}} - I_{\text{dark}}$,^{21,22} increases as the applied bias voltage increases. The observed phenomena can be explained by the carrier transit time dependence on bias voltage as, carrier transit time $t = L^2/(\mu \times V_b)$, where L is the channel length of the device, μ is the carrier mobility, and V_b is the applied bias voltage.²³ A similar behavior has recently been reported for the MoS_2 nanowire-based UV detector.²⁴

To calculate the rise and decay times of the three devices at low bias voltage of 0.5 V, three-single cycle from each device has been used, as demonstrated in Fig. 4(b). The rise time (t_r) is defined as the time required for the photocurrent to increase from 10% to 90% of its saturation value, whereas the decay time (t_d) is the time required for the photocurrent to decrease from 90% to 10% of its saturation value. Based on this definition, the photodetectors revealed rise and decay times of 0.687 and 0.747 s for the 120-nm channel length device, 0.784 and 0.853 s



(a)



(b)

Fig. 2 (a) SEM images of the SiCNW-UVPD devices with multiple electrodes with spacing of 120 to 460 nm from right to left, respectively, and 800 nm (bottom inset) on a highly doped SiO₂/Si substrate (scale bar is 10 μm). (b) A schematic view of the measurement setup.

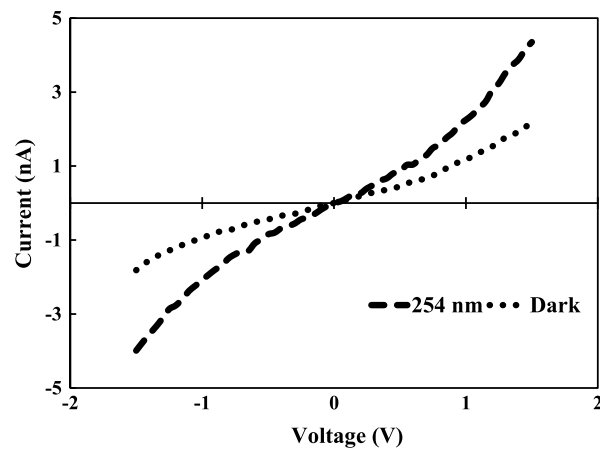


Fig. 3 *I*-*V* characteristics of the SiCNW-UVPD device with 120-nm channel length both in absence (dark) and presence (with light) of 254-nm UV illumination. The device presents high sensitivity to the UV light with significant increase in photocurrent under 254-nm UV exposure.

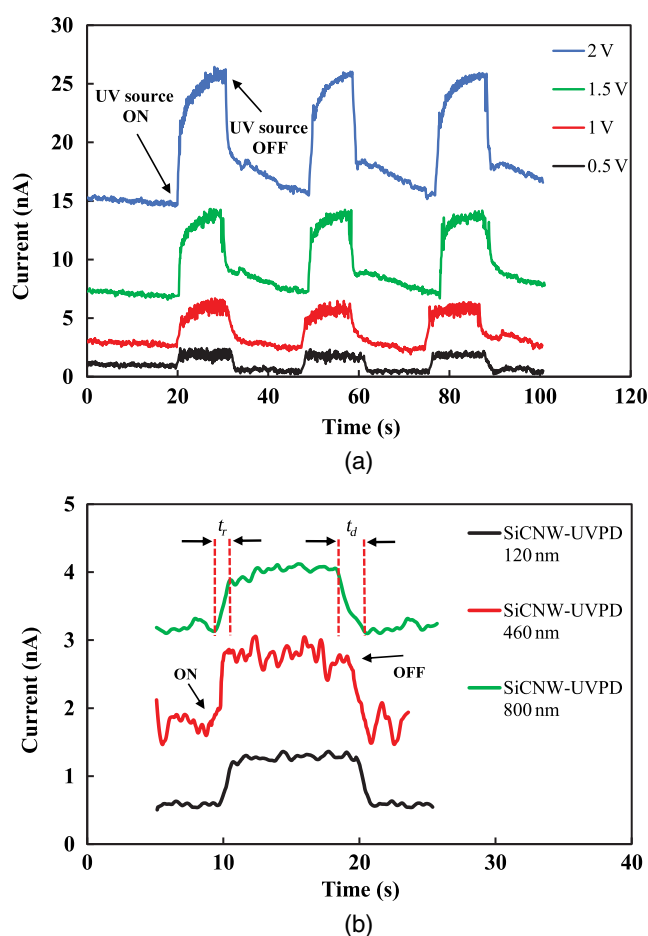


Fig. 4 (a) Photocurrent-time responses of the SiCNW-UVPD device with 120-nm channel length under different bias voltages of 0.5, 1, 1.5, and 2 V. The UV source was kept ON for 10 s and OFF for 20 s with three consecutive cycles. (b) Three single cycle from each device at 0.5 V for the calculation of the rise and decay times. The rise and decay times are 0.687 and 0.747 s, respectively, for the fastest device with the shortest channel length of 120 nm.

for the 460-nm channel length device, and 0.833 and 0.924 s for the 800-nm channel length device, respectively, at bias voltage of 0.5 V. In fact, these results indicate a considerable improvement on the speed of the SiCNW-UVPD devices compared to the earlier reports with the rise times ranging from 3 to 14 s.^{10,11}

To investigate the impact of channel length scaling on the photodetector sensitivity, which is defined as $S = (I_{\text{ph}}/I_{\text{dark}}) \times 100$,^{25,26} where I_{ph} is the photocurrent and I_{dark} is the dark current, the sensitivity of UV photodetector devices with channel length of 120, 460, and 800 nm has been calculated at the same bias voltage. We observed that as the channel length gets longer, the sensitivity of the photodetector gradually decreases. The measured sensitivity of the SiCNW-UVPDs at 0.5-V bias is 90.8, 47.0, and 43.2 with channel lengths of 120, 460, and 800 nm, respectively. The similar trend at different bias voltages of 1.0, 1.5, and 2.0 V has been observed in all devices, as presented in Table 1.

In addition to the speed of a photodetector, responsivity (R_{λ}), EQE, and responsivity–bandwidth product are considered to be key performance parameters. Responsivity indicates the ratio of generated photocurrent to incident power on irradiated area and is expressed by $R_{\lambda} = I_{\lambda}/(P_{\lambda} \times A)$, where I_{λ} is the photocurrent, P_{λ} is the power density, and A is the effective exposed area of the device, $A = 2\pi rL/2$.^{27–29} EQE indicates the number of charge carriers created per incident photon and is expressed as $\text{EQE} = h \times c \times R_{\lambda}/(e \times \lambda)$, where h , c , R_{λ} , e , and λ are the Planck's constant, light velocity, responsivity, electron charge, and the wavelength of excitation UV light,^{30,31} respectively. The high values of R_{λ} and EQE demonstrate high

Table 1 Comparison of the sensitivity of the three different SiCNW-UVPDs with channel lengths of 120, 460, and 800 nm at various bias voltages of 0.5, 1.0, 1.5, and 2.0 V. The sensitivity decreases as the channel length increases at constant bias voltage.

Channel length (nm)	Sensitivity at different bias voltage (V)			
	0.5	1.0	1.5	2.0
120	90.8	122.9	117.2	127.1
460	47.0	53.7	91.6	71.6
800	43.2	20.8	28.0	41.9

sensitivity to UV light. In fact, our measurements revealed very high values of R_λ and EQE as 7.73×10^3 A/W and $7.77 \times 10^4\%$, respectively, to the 254-nm UV light exposure at bias voltage of 0.5 V. Furthermore, another important photodetector metric, responsivity–bandwidth product, has been determined. The bandwidth for the devices was calculated by $BW = 1/(2\pi t_{rise})$.³²

Our achieved values at the bias voltage of 0.5 V and the channel length of 120 nm are the highest values compared to the reported SiC and other semiconductor photodetectors operating at even higher bias voltages. Table 2 presents a comprehensive comparison of the some key performance parameters (rise and decay time, responsivity, EQE, and responsivity–bandwidth product) of the SiCNW-UVPDs with the channel length of 120, 460, and 800 nm along with some other photodetectors. The achieved responsivity values of the SiCNW-UVPDs with 120-, 460-, and 800-nm channel length are 7.73×10^3 A/W, 5.41×10^3 A/W, and 4.89×10^3 A/W, respectively, at bias voltage of 0.5 V. Similarly, the achieved EQE values of the SiCNW-UVPDs with 120-, 460-, and 800-nm channel length are $7.77 \times 10^4\%$, $2.64 \times 10^4\%$, and $2.38 \times 10^4\%$, respectively, at bias voltage of 0.5 V. In addition to the very high responsivity of our SiCNW-UVPDs, the responsivity slightly decreases with the increase in channel length, which is likely due to the increase in effective exposed area of the device (A). A similar trend can be seen with the EQE, which is likely due to dependence on the responsivity, as the channel length increases.

Based on these R_λ , EQE, and responsivity–bandwidth product performance metrics, our devices operating at lower voltage exhibit significantly better performance than that of the other devices operating at higher voltages (see Table 2). Figure 5(a) presents the plot of the channel length dependence of the responsivity and EQE of the three SiCNW-UVPDs. Moreover, the

Table 2 Comparison of the some key performance parameters (rise and decay time, responsivity, EQE, and responsivity–bandwidth product) of the SiCNW-UVPDs with the channel length of 120, 460, and 800 nm along with some other photodetectors.

Material	Rise time (s)	Decay time (s)	Current responsivity (R_λ) (A/W)	EQE (%)	Gain mechanism	$R_\lambda \times BW$	Channel length (nm)	Bias voltage (V)	Reference
ZnO-NW	9.5	38	0.43	0.24×10^4	Photocond.	0.0711	3×10^6	5	7
GaN-NW	—	—	70.4	~100	Photocond.	—	0.2×10^6	5	8
In ₂ Se ₃ -NW	~0.3	~0.3	~89	2.2×10^4	Photocond.	446.0	1×10^3	3	9
SiC film	14	—	0.18	86	Photocond.	0.0202	—	10	10
SiCNW	3	5	—	—	Photocond.	—	3×10^3	2	11
TiO ₂ -NW	2.5	10	90	—	Photocond.	56.548	$\sim 8 \times 10^3$	10	16
SiCNW	0.687	0.747	7.73×10^3	7.77×10^4	Photocond.	77.6×10^3	120	0.5	This work
SiCNW	0.784	0.853	5.41×10^3	2.64×10^4	Photocond.	10.8×10^3	460	0.5	This work
SiCNW	0.833	0.924	4.89×10^3	2.38×10^4	Photocond.	9.22×10^3	800	0.5	This work

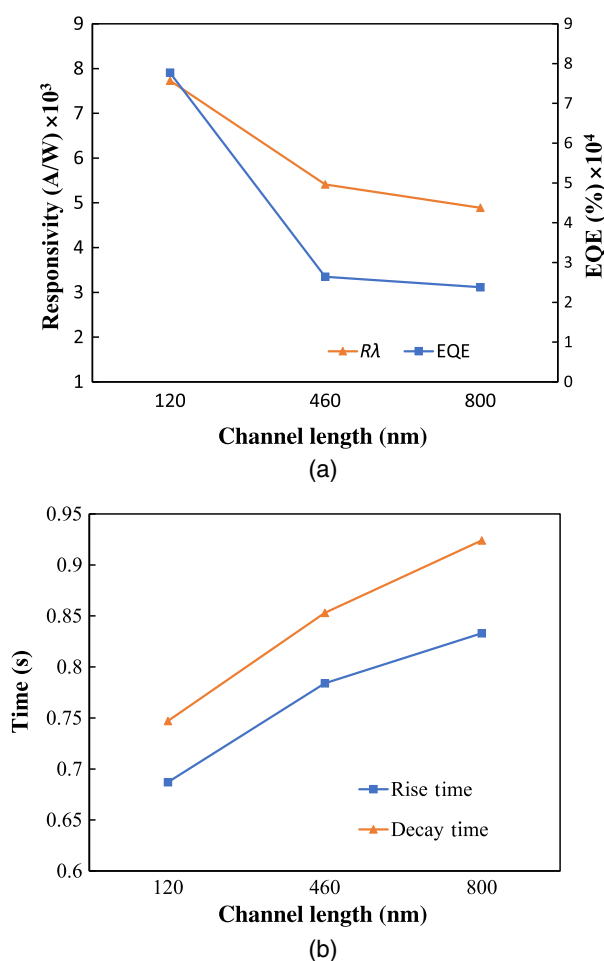


Fig. 5 The channel length dependence of the (a) $R\lambda$ and EQE. (b) Rise and decay time values of the SiCNW-UVPDs with 120-, 460-, and 800-nm channel length at 0.5-V bias.

channel length dependence of the speed of the SiCNW-UVPDs is shown in Fig. 5(b). As the channel length gets longer, an increase in rise and decay time values of the SiCNW-UVPDs can be seen.

The increase in rise and decay times could be due to the increase in carrier transit time with the increase in channel length. Similar trend in rise and decay times with the increase in channel length has been observed in a study on CdS thin film photodetector device.³³ Consequently, significantly better performance of the SiCNW-UVPDs at low operating voltage can open the possibilities of the development of high-speed and sensitive photodetector devices for emerging nanophotonic and nanoelectronic applications with low power consumption.

4 Conclusions

We have successfully demonstrated the channel length dependence of the key performance parameters, such as speed, responsivity, EQE, and responsivity–bandwidth product, of the SiCNW-UVPDs with different channel lengths ranging from 120 to 800 nm. The SiCNW-UVPDs have shown very good performance even at low operating voltage of 0.5 V. Furthermore, the SiCNW-UVPD with the shortest channel of 120 nm exhibited the best performance values with the rise time of 0.687 s, decay time of 0.747 s, responsivity of 7.73×10^3 A/W, and EQE of $7.77 \times 10^4\%$ at a low operating voltage of 0.5 V. This study shows that scaling down in channel length improves the performance of the photodetector. As a consequence, significantly better performance of the SiCNW-UVPDs at low operating voltage open the possibilities of the

development of high-speed and sensitive photodetector devices for emerging optoelectronic and nanoelectronic applications with low power consumption.

Acknowledgments

The authors gratefully thank to the Marie Curie FP7 Integration Grant within the 7th European Union Framework Program and Istanbul Development Agency (ISTKA) for providing support for this research.

References

1. Y. Cui et al., "High performance silicon nanowire field effect transistors," *Nano Lett.* **3**(2), 149–152 (2003).
2. J. Choi et al., "Comparison of bottom-up and top-down 3C-SiC NWFETs," *Mater. Sci. Forum* **858**, 1001–1005 (2016).
3. C. Battaglia et al., "Enhanced near-bandgap response in InP nanopillar solar cells," *Adv. Energy Mater.* **4**, 1400061 (2014).
4. P. Yu et al., "Design and fabrication of silicon nanowires towards efficient solar cells," *Nano Today* **11**(6), 704–737 (2016).
5. D. Lin, H. Wu, and W. Pan, "Photoswitches and memories assembled by electrospinning aluminum-doped zinc oxide single nanowires," *Adv. Mater.* **19**, 3986–3972 (2007).
6. J. R. Kim et al., "Schottky diodes based on a single GaN nanowire," *Nanotechnology* **13**, 701–704 (2002).
7. B. D. Boruah et al., "Highly dense ZnO nanowires grown on graphene foam for ultraviolet photodetection," *ACS Appl. Mater. Interfaces* **7**(19), 10606–10611 (2015).
8. W. Y. Weng et al., "A high-responsivity GaN nanowire UV photodetector," *IEEE J. Sel. Top. Quantum Electron.* **17**(4), 996–1001 (2011).
9. T. Zhai et al., "Fabrication of high-quality In₂Se₃ nanowire arrays toward high-performance visible-light photodetectors," *ACS Nano* **4**(3), 1596–1602 (2010).
10. A. Aldalbahi et al., "A new approach for fabrications of SiC based photodetectors," *Sci. Rep.* **6**, 23457 (2016).
11. K. Teker, "Photoresponse characteristics of silicon carbide nanowires," *Microelectron. Eng.* **162**, 79–81 (2016).
12. H. Chen et al., "New concept ultraviolet photodetectors," *Mater. Today* **18**(9), 493–502 (2015).
13. E. Monroy, F. Omnes, and F. Calle, "Wide-bandgap semiconductor ultraviolet photodetectors," *Semicond. Sci. Technol.* **18**(4), R33–R51 (2003).
14. D. Prasai et al., "Highly reliable silicon carbide photodiodes for visible-blind ultraviolet detector applications," *J. Mater. Res.* **28**(1), 33–37 (2012).
15. B. Mallampati et al., "Role of surface in high photoconductive gain measured in ZnO nanowire-based photodetector," *J. Nanopart. Res.* **17**(4), 176 (2015).
16. A. J. Molina-Mendoza et al., "Highly responsive UV-photodetectors based on single electrospun TiO₂ nanofibres," *J. Mater. Chem. C* **4**, 10707–10714 (2016).
17. F. Liu et al., "Investigation on the photoconductive behaviors of an individual AlN nanowire under different excited lights," *Nanoscale Res. Lett.* **7**(1), 454 (2012).
18. W. S. Ko et al., "Ultrahigh responsivity-bandwidth product in a compact InP nanopillar phototransistor directly grown on silicon," *Sci. Rep.* **6**, 33368 (2016).
19. R. W. Going et al., "Germanium gate PhotoMOSFET integrated to silicon photonics," *IEEE J. Sel. Top. Quantum Electron.* **20**, 8201607 (2014).
20. A. Uzun and K. Teker, "Silicon carbide nanowire field effect transistors with high on/off current ratio," *Microelectron. Eng.* **205**, 59–62 (2019).
21. W. Zhang et al., "Ultrahigh-gain photodetectors based on atomically thin graphene-MoS₂ heterostructures," *Sci. Rep.* **4**, 3826 (2014).
22. X. Liu et al., "All-printable band-edge modulated ZnO nanowire photodetectors with ultrahigh detectivity," *Nat. Commun.* **5**, 4007 (2014).

23. A. Sharma et al., "High performance broadband photodetector using fabricated nanowires of bismuth selenide," *Sci. Rep.* **6**, 19138 (2016).
24. O. Lopez-Sanchez et al., "Ultrasensitive photodetectors based on monolayer MoS₂," *Nat. Nanotechnol. Lett.* **8**(7), 497–501 (2013).
25. F. H. Alsultany, Z. Hassan, and N. M. Ahmed, "A high-sensitivity, fast-response, rapid-recovery UV photodetector fabricated based on catalyst-free growth of ZnO nanowire networks on glass substrate," *Opt. Mater.* **60**, 30–37 (2016).
26. A. M. Selman and Z. Hassan, "Highly sensitive fast-response UV photodiode fabricated from rutile TiO₂ nanorod array on silicon substrate," *Sens. Actuators, A* **221**, 15–21 (2015).
27. T. Ueda et al., "Charge-sensitive infrared phototransistors: characterization by an all-cryogenic spectrometer," *J. Appl. Phys.* **103**, 093109 (2008).
28. J. M. Wu and W. E. Chang, "Ultrahigh responsivity and external quantum efficiency of an ultraviolet-light photodetector based on a single VO₂ microwire," *ACS Appl. Mater. Interfaces* **6**(16), 14286–14292 (2014).
29. C. Soci et al., "Nanowire photodetectors," *J. Nanosci. Nanotechnol.* **10**, 1430–1449 (2010).
30. S. Almazan et al., "Extreme UV photodetectors based on CVD single crystal diamond in a p-type/intrinsic/metal configuration," *Diamond Relat. Mater.* **18**, 101–105 (2009).
31. X. Zhang et al., "Ultrasensitive and highly selective photodetections of UV-A rays based on individual bicrystalline GaN nanowire," *ACS Appl. Mater. Interfaces* **9**, 2669–2677 (2017).
32. C. Soci et al., "ZnO nanowire UV photodetectors with high internal gain," *Nano Lett.* **7**, 1003–1009 (2007).
33. A. Sharma et al., "Channel length specific broadspectral photosensitivity of robust chemically grown CdS photodetector," *AIP Adv.* **5**, 047116 (2015).

Ali Uzun is a graduate student at Istanbul Sehir University, Electrical and Computer Engineering Program. His current research interests include fabrication and testing of silicon carbide nanowire-based devices.

Kasif Teker is a professor at Istanbul Sehir University. He received his MS and PhD degrees in materials science from the Ohio State University in 1996 and Case Western Reserve University in 2001, respectively. Following his PhD, he has worked in compound semiconductor industry as a scientist for three years in USA. He has worked as a faculty member in the Physics and Engineering Department, Frostburg State University, Maryland, USA, for eight years. His current research interests include fabrication and testing of nanoelectronic and nanophotonic devices.